

Cite this: *Chem. Sci.*, 2021, 12, 3239

All publication charges for this article have been paid for by the Royal Society of Chemistry

# A [3Cu:2S] cluster provides insight into the assembly and function of the Cu<sub>Z</sub> site of nitrous oxide reductase†

Lin Zhang,<sup>a</sup> Eckhard Bill,<sup>b</sup> Peter M. H. Kroneck<sup>c</sup> and Oliver Einsle<sup>b,\*a</sup>

Nitrous oxide reductase (N<sub>2</sub>OR) is the only known enzyme reducing environmentally critical nitrous oxide (N<sub>2</sub>O) to dinitrogen (N<sub>2</sub>) as the final step of bacterial denitrification. The assembly process of its unique catalytic [4Cu:2S] cluster Cu<sub>Z</sub> remains scarcely understood. Here we report on a mutagenesis study of all seven histidine ligands coordinating this copper center, followed by spectroscopic and structural characterization and based on an established, functional expression system for *Pseudomonas stutzeri* N<sub>2</sub>OR in *Escherichia coli*. While no copper ion was found in the Cu<sub>Z</sub> binding site of variants H129A, H130A, H178A, H326A, H433A and H494A, the H382A variant carried a catalytically inactive [3Cu:2S] center, in which one sulfur ligand, S<sub>Z2</sub>, had relocated to form a weak hydrogen bond to the sidechain of the nearby lysine residue K454. This link provides sufficient stability to avoid the loss of the sulfide anion. The UV-vis spectra of this cluster are strikingly similar to those of the active enzyme, implying that the flexibility of S<sub>Z2</sub> may have been observed before, but not recognized. The sulfide shift changes the metal coordination in Cu<sub>Z</sub> and is thus of high mechanistic interest.

Received 20th September 2020

Accepted 3rd January 2021

DOI: 10.1039/d0sc05204c

rsc.li/chemical-science

## Introduction

Nitrous oxide (N<sub>2</sub>O) is an inert, odorless and non-toxic gas that nevertheless acts as a greenhouse agent with a global warming potential exceeding that of carbon dioxide (CO<sub>2</sub>) by a factor of 300.<sup>1</sup> Its atmospheric concentration is on a steady rise, at a rate of 0.2–0.3% per year,<sup>1,2</sup> which led to its designation as the most significant ozone-depleting substance of the 21<sup>st</sup> century.<sup>3</sup> The biological reduction of N<sub>2</sub>O is catalyzed exclusively by nitrous oxide reductase (N<sub>2</sub>OR) as the ultimate step of the bacterial metabolic pathway of denitrification.<sup>2</sup> N<sub>2</sub>OR is a periplasmic metalloprotein of 130 kDa that contains two copper centers, Cu<sub>A</sub> and Cu<sub>Z</sub>, in each monomer. Midpoint reduction potentials and spectroscopic properties of the two centers are distinct and provide detailed information about the respective electronic state of the sites.<sup>4–6</sup> The three-dimensional structures of N<sub>2</sub>OR from *Marinobacter hydrocarbonoclasticus* (PDB 1QNI),<sup>7</sup> *Paracoccus denitrificans* (PDB 1FWX),<sup>8</sup> *Achromobacter cycloclastes* (PDB 2IWF),<sup>9</sup> *Pseudomonas stutzeri* (PDB 3SBQ),<sup>10</sup> and *Shewanella denitrificans* (PDB 5I5M)<sup>11</sup> were reported, providing structural details for various states of the copper centers. The

dimeric N<sub>2</sub>OR forms a tight head-to-tail arrangement that juxtaposes the Cu<sub>A</sub> site of one monomer with the Cu<sub>Z</sub> site of the other, placing the two sites in sufficient proximity (10 Å) to form the composite active site of the enzyme at each dimer interface.<sup>7,8</sup> Cu<sub>A</sub> is a binuclear mixed-valent [Cu<sup>1.5+</sup>:Cu<sup>1.5+</sup>] site<sup>12,13</sup> liganded by one methionine, one tryptophan, two cysteines and two histidines that is found in a very similar form in many respiratory heme:copper oxidases,<sup>14</sup> and it mediates one-electron transfer at a midpoint potential of approximately +260 mV vs. SHE.<sup>6,15,16</sup> When isolated under anoxic conditions – a state referred to as ‘form I’<sup>17</sup> – the Cu<sub>Z</sub> site that binds N<sub>2</sub>O is a tetranuclear [4Cu:μ<sub>4</sub>-S:μ<sub>2</sub>-S] cluster coordinated by seven histidines, as has been demonstrated for *M. hydrocarbonoclasticus* N<sub>2</sub>OR<sup>18</sup> and *P. stutzeri* N<sub>2</sub>OR.<sup>10</sup> The Cu<sub>Z</sub> site seems to be prone to decomposition, losing sulfide ligand S<sub>Z2</sub> to yield a [4Cu:μ<sub>4</sub>-S] site designated Cu<sub>Z</sub>\* in an enzyme referred to as form II.<sup>19,20</sup> Notably, a conclusion of the present discussion will be that these terms require re-definition. In other structural analyses, Cu<sub>Z</sub> sites were modelled to contain either a μ<sub>2</sub>-bridging water molecule, two terminal waters or an iodide anion that acted as an inhibitor, adding to a lack of clarity regarding the relevant active forms of this site.<sup>7–9,20</sup>

To date, understanding of the biogenesis of Cu<sub>Z</sub> remains fragmentary, but a series of maturation factors involved in the process have been identified.<sup>5</sup> Interestingly, the apoenzyme is exported as a folded dimer *via* the Tat pathway, although the entire maturation of the metal sites occurs in the periplasm.<sup>21</sup> Here the dedicated metallochaperone NosL, a lipoprotein,

<sup>a</sup>Institut für Biochemie, Albert-Ludwigs-Universität Freiburg, Albertstrasse 21, 79104 Freiburg im Breisgau, Germany. E-mail: einsle@biochemie.uni-freiburg.de

<sup>b</sup>Max-Planck-Institut für Chemische Energiekonversion, Stiftstr. 34-36, D-45470 Mülheim an der Ruhr, Germany

<sup>c</sup>Fachbereich Biologie, Universität Konstanz, 78457 Konstanz, Germany

† Electronic supplementary information (ESI) available. See DOI: 10.1039/d0sc05204c



binds  $\text{Cu}^+$  and delivers it to apo- $\text{N}_2\text{OR}$ ,<sup>22</sup> and a recent study has suggested its role to be in particular for  $\text{Cu}_Z$  site assembly.<sup>23</sup>

In addition, the ABC transporter NosFY in conjunction with the periplasmic NosD protein is required to provide a sulfur species to the periplasm in order to complete  $\text{Cu}_Z$  maturation.<sup>17</sup> We recently established a recombinant system that included all essential genes *nosRZDFYLX* for  $\text{N}_2\text{OR}$  production, able to generate functional enzyme containing both  $\text{Cu}_A$  and  $\text{Cu}_Z$  sites in *E. coli*,<sup>24</sup> facilitating mutagenesis studies of the key residues coordinating the copper sites.

## Results and discussion

### Properties of the seven histidine variants of $\text{Cu}_Z$

In the present study we focus on understanding the role of the seven ligands of the  $\text{Cu}_Z$  site, namely H129, H130, H178, H326, H382, H433 and H494 of *P. stutzeri*  $\text{N}_2\text{OR}$  ( $\text{PsN}_2\text{OR}$ ). All histidine residues were individually mutated to alanine. The corresponding variants were purified (Fig. S1†), followed by spectroscopic characterization and the determination of three-dimensional structures by X-ray crystallography (Table S1†).

Not unexpectedly, six of the seven variants of the coordinating histidine residues, namely H129A, H130A, H178A, H326A, H433A and H494A only showed spectral properties confirming the presence of the  $\text{Cu}_A$  site (Fig. S2†), with absorption maxima at 485 nm, 525 nm and 795 nm, although the relative occupancy of  $\text{Cu}_A$  was found to differ (Table S2†). However, the H382A variant showed UV-vis spectra that were nearly identical to those of wild-type  $\text{N}_2\text{OR}$  (Fig. 1). The oxically isolated H382A was of blue colour, with partially oxidized copper sites as indicated by comparing the spectra of sample as isolated (Fig. 1D, blue) and ascorbate-reduced (Fig. 1E, blue).

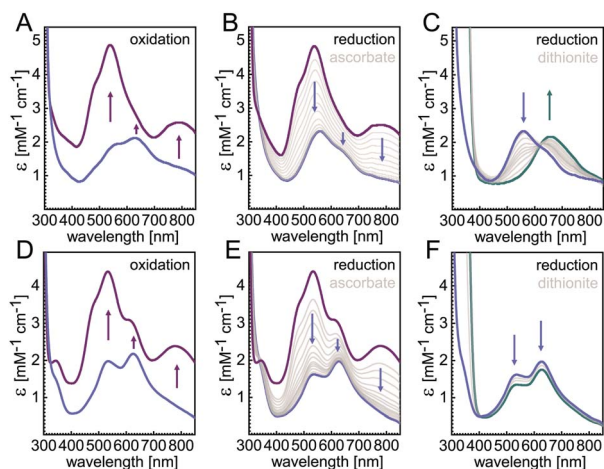


**Fig. 1** UV-vis spectra of WT  $\text{PsN}_2\text{OR}$  (A–C) and variant H382A (D–F). As isolated, H382A (D) showed two absorption peaks at 535 nm and 625 nm (blue); upon oxidation with ferricyanide the spectra (purple) were similar to the wild type form I  $\text{N}_2\text{OR}$  (A). (B and E) Selective reduction of  $\text{Cu}_A$  with ascorbate yielded a two-peak spectrum indicative of a  $[\text{4Cu:2S}]$   $\text{Cu}_Z$  site (blue). Upon extended reduction with dithionite, the typical loss of the 535 nm band seen for WT  $\text{PsN}_2\text{OR}$  (C) was not observed in the H382A (F) variant (cyan).

After oxidation with ferricyanide the protein underwent a colour change to purple, with absorption maxima at 533 nm and 780 nm and two prominent shoulders at 485 nm and 625 nm (Fig. 1D, purple). These features do not merely reflect a mixed-valent  $\text{Cu}_A$  site, but correspond to the properties of a wild-type form I  $\text{N}_2\text{OR}$  (Fig. 1A),<sup>6,25,26</sup> except for the more pronounced shoulder peak at 625 nm. The selective reduction of  $\text{Cu}_A$  by ascorbate resulted in two distinct bands at 535 nm and 625 nm (Fig. 1E, blue). We have earlier described this two-peak spectrum of  $\text{Cu}_Z$  as a signature of the  $[\text{4Cu:2S}]$  form I, with the 625 nm maximum originating from  $\text{S}_{Z1}$  and the second peak, found at 562 nm in wild-type  $\text{N}_2\text{OR}$ , as originating from  $\text{S}_{Z2}$ ,<sup>10</sup> although a difference assignment attributing this transition to also originate from  $\text{S}_{Z1}$  was made by other.<sup>18</sup> The spectrum of H382A  $\text{N}_2\text{OR}$  thus indicated that – unlike in  $\text{Cu}_Z^*$  – sulfide  $\text{S}_{Z2}$  was still present, but the shifted peak indicated a change in its chemical environment. Also, the intensity ratio of the two  $\text{Cu}_Z$  bands indicated an incomplete occupancy for  $\text{S}_{Z2}$ . Intriguingly, further reduction with dithionite did not lead to a loss of either band (Fig. 1F, cyan), indicating the “ $\text{Cu}_Z$ ” site in H382A was redox-inert. In wild-type  $\text{N}_2\text{OR}$ , dithionite reduction leads to a single charge transfer peak at 650 nm (Fig. 1C), which was assigned to the reduction of  $\text{Cu}_Z$  from a  $[\text{2Cu}^+:\text{2Cu}^{2+}]$  state to a  $[\text{3Cu}^+:\text{1Cu}^{2+}]$  form.<sup>4,18,27</sup> We then determined the  $\text{N}_2\text{O}$ -reducing activity using reduced benzyl viologen as electron donor. H382A was not active in  $\text{N}_2\text{O}$  reduction (Fig. S3F†). We also determined the specific activities for the other six variants, and while H129A, H130A, H326A, H433A and H494A were completely inactive as expected (Fig. S3†), H178A showed low activity, with a decrease in  $v_{\text{max}}$  to  $0.03 \pm 0.01 \mu\text{mol N}_2\text{O}$  per min per mg, approximately 50-fold lower than that of wild-type enzyme,<sup>24</sup> and  $K_M$  ( $\text{N}_2\text{O}$ ) of  $268 \pm 24 \mu\text{M}$  (Fig. S3D†). This residual activity (validated by 3 replicates) might be originated from a small portion of H178A containing a functional  $\text{Cu}_Z$  site, but the overall occupancy of possibly only 2% given the 50-fold lower activity was too low to be observed in the UV-vis spectra and crystal structure (*vide infra*).

We further proceeded to crystallize all variants and determined their three-dimensional structures to resolutions ranging from 1.67 Å to 1.49 Å (Table S3 and Fig. S4–S11†). As expected, the overall fold and dimeric structure of all variants remained unchanged,<sup>24</sup> with root-mean-squared deviations for all atoms from wild-type  $\text{N}_2\text{OR}$  at 0.34 Å (H129A), 0.28 Å (H130A), 0.14 Å (H178A), 0.48 Å (H326A), 0.11 Å (H382A), 0.32 Å (H433A), and 0.23 Å (H494A). Overall, the major structural difference was that the  $\text{Ca}^{2+}$ -binding loop (N257–D273) was disordered in some of variants. This disorder seemed to correlate with the occupancy of the  $\text{Cu}_A$  site (Tables 1 and S2†), in line with an early report that the presence of  $\text{Ca}^{2+}$  ions was required for a stable insertion of the center.<sup>11</sup>

Although at different occupancies, the  $\text{Cu}_A$  site was present in all seven-variants (Table S2 and Fig. S4–S11†). The  $\text{Cu}_A$  ligands C618, W620, C622, H626, and M629 were in place to coordinate two copper ions, but the remaining ligand, H583, was in one of two possible conformations (*e.g.* Fig. S4†). In a ‘bound’ conformation, the  $\text{N}_\delta$  atom of the imidazole moiety coordinated  $\text{Cu}_{A1}$  at a distance of 2.5 Å, and the  $\text{N}_\epsilon$  atom formed



**Table 1** Structural information on WT *PsN<sub>2</sub>OR* the seven histidine variants

Variant	Side <sup>a</sup>	Ca <sup>2+</sup> -binding loop	Cu <sub>Z</sub>	Cu <sub>A</sub> -His583 <sup>b</sup>		
WT <sup>c</sup>	A	Ordered	[4Cu:2S]	Unbound	3.74 Å	
	B	Ordered	[4Cu:2S]	Unbound	3.44 Å	
H129A	A	Ordered	Empty	Bound	2.51 Å	
	B	Disordered	1 Zn <sup>2+</sup>	Unbound	3.46 Å	
H130A	A	Ordered	Empty	Unbound	3.49 Å	
	B	Disordered	Empty	Unbound	3.84 Å	
H178A	A	Ordered	Empty	Bound	2.33 Å	
	B	Ordered	Empty	Bound	2.46 Å	
H326A	A	Disordered	1 Zn <sup>2+</sup>	Unbound	3.93 Å	
	B	Disordered	1 Zn <sup>2+</sup>	Unbound	3.86 Å	
H382A	A	Ordered	[3Cu:2S]	Unbound	3.69 Å	
	B	Ordered	[3Cu:2S] <sup>d</sup>	Unbound	3.68 Å	
H433A	A	Ordered	Empty	Unbound	3.47 Å	
	B	Disordered	Empty	Unbound	3.85 Å	
H494A	A	Ordered	1 Zn <sup>2+</sup>	Bound	2.82 Å	
	B	Disordered	2 Zn <sup>2+</sup>	Unbound	3.29 Å	

<sup>a</sup> Side A shows Cu<sub>A</sub> of chain A, Ca<sup>2+</sup>-binding loop and Cu<sub>Z</sub> of chain B, which together form one active site; side B means the other way around. <sup>b</sup> Cu<sub>A</sub> is present in all seven variants. 'Bound' indicates H583 is a ligand of Cu<sub>A1</sub>, while 'unbound' means it is turned away. The given distances are between Cu<sub>1</sub> and H583; see Table S4 for more details. <sup>c</sup> PDB accession code 6RL0. <sup>d</sup> Chain A of H382A shows weak density for Cu<sub>1</sub> in the Cu<sub>Z</sub> site. See Fig. S9B for more details.

a short hydrogen bond (2.7 Å) to residue D576 (Fig. S4A†). This is a state for Cu<sub>A</sub><sup>28</sup> that is most commonly observed and was also found in N<sub>2</sub>OR of *M. hydrocarbonoclasticus*,<sup>7</sup> *P. denitrificans*,<sup>8</sup> and *A. cycloclastes*,<sup>9</sup> as well as in cytochrome *c* oxidases (PDB ID: 2CUA).<sup>29</sup> In the second, 'unbound' state, however, the imidazole group of H583 was rotated away from Cu<sub>A</sub> by approximately 135°, so that the N<sub>δ</sub> atom now formed a hydrogen bond to residue S550, while the H-bond between N<sub>ε</sub> atom and D576 remained unchanged (Fig. S4B†). This histidine flip at Cu<sub>A</sub> was previously reported for *P. stutzeri* N<sub>2</sub>OR,<sup>10</sup> and we proposed a role in gating electron transfer from an external redox partner to Cu<sub>A</sub>.<sup>20</sup> In our previous study, H583 showed only partial ligation of Cu<sub>A</sub> in either form I and II of recombinant *PsN<sub>2</sub>OR*.<sup>24</sup> However, the conformational switch of H583 was randomly distributed among the variants (Table 1). Geometry changes of Cu<sub>A</sub> were also observed between the two conformations of H583. The major difference was that the bond lengths of Cu<sub>A2</sub> to the sulfur atoms of C618 and C622 were about 0.1 Å longer when H583 was not a ligand (Table S4†).

The UV-vis spectra of the six variants H129A, H130A, H178A, H326A, H433A and H494A lacked the S → Cu charge transfer bands typically associated with the Cu<sub>Z</sub> center (Fig. S2†). This is primarily indicative of an absence of sulfide, but the presence of histidine-coordinated Cu alone should also lead to similar N → Cu CT bands, albeit with lower intensity. Only the H326A variant might show such a peak at 630 nm (Fig. S2D†), while the other five gave no indication for the presence of Cu. Structural analysis revealed that in the variants H130A, H178A and H433A the Cu<sub>Z</sub> site was only occupied by water molecules (Fig. S5, S6 and S10†). In the H129A, H326A and H494A variants, one or two zinc ions were instead found at the binding site for Cu<sub>Z</sub> (Fig. S4,

S7 and S11†), as confirmed by anomalous scattering data collected at the X-ray absorption K-edge of Zn (9700 eV). The presence of Zn<sup>2+</sup> in the Cu<sub>Z</sub> site can be rationalized by non-specific incorporation *via* a periplasmic zinc chaperone such as ZinT<sup>30</sup> or ZraP,<sup>31,32</sup> and the presence of multiple histidines, which are suitable ligands for zinc.<sup>33</sup> The metal might occupy this site if the regular Cu<sub>Z</sub> maturation pathway is dysfunctional. Note that in no case either a single or two Cu ions were observed. Since the maturation factors NosDFYL were present for the production of all N<sub>2</sub>OR variants in *E. coli*, copper (and sulfide) delivery should have been possible. The complete lack of Cu thus either means that each of the six histidines mutated here is essential for assembly, or that any site assembled without the full complement of ligands is unstable and the metal is quickly lost.

### A [3Cu:2S] cluster in the H382A variant

The unexpected UV-vis spectra (Fig. 1D) were reflected in an unprecedented, only partially assembled [3Cu:μ<sub>3</sub>S:μ-S] cluster at the Cu<sub>Z</sub> site (Fig. 2B). In this cluster, Cu<sub>1</sub> was absent, leaving S<sub>Z1</sub> as a μ<sub>3</sub>-bridging sulfide ligating the remaining three copper ions. The histidine coordination of these was identical to native Cu<sub>Z</sub>, in that Cu<sub>2</sub> was coordinated by H129 and H178, Cu<sub>3</sub> by H130 and H433, and Cu<sub>4</sub> by H494. Furthermore, the second sulfide, S<sub>Z2</sub>, was still present as a ligand to Cu<sub>4</sub>, in spite of the absence of Cu<sub>1</sub>. It shifted position towards the nearby lysine K454, forming a hydrogen bond that stabilized the [3Cu:2S] cluster (Fig. 3B). As a consequence, the S<sub>Z1</sub>-Cu<sub>4</sub>-S<sub>Z2</sub> bond angle in the [3Cu:2S] site increased by approximately 26° with respect to the one in the native, [4Cu:2S] Cu<sub>Z</sub>. In contrast, the changes to the individual bond lengths in the cluster were insignificant (Fig. 3C).

The X-band EPR spectra for both WT N<sub>2</sub>OR (Fig. 4A) and H382A variant (Fig. 4D) showed a similar 7-line hyperfine splitting pattern in the *g*<sub>||</sub> region originating from the mixed-valent [Cu<sup>1.5+</sup>:Cu<sup>1.5+</sup>] state of oxidized Cu<sub>A</sub>,<sup>12,14</sup> although the

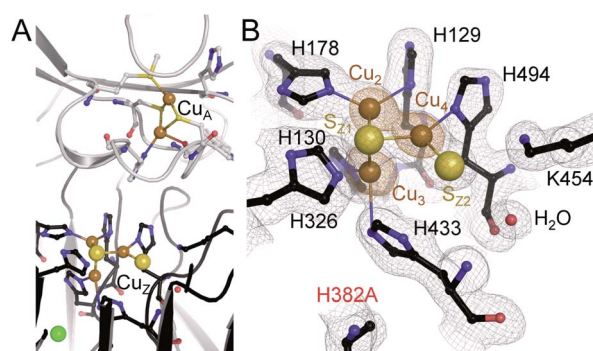


**Fig. 2** Characterization of the *PsN<sub>2</sub>OR* variant H382A. (A) The three-dimensional structure of H382A shows the presence of binuclear Cu<sub>A</sub> site, while Cu<sub>Z</sub> is an incomplete [3Cu:2S] cluster due to the loss of copper atom Cu<sub>Z1</sub>. (B) Electron density map around the [3Cu:2S] site. The grey map is a 2F<sub>o</sub> - F<sub>c</sub> electron density map contoured at the 1σ level, and anomalous difference Fourier maps (data collected at the X-ray absorption edge of Cu, 9050 eV) are shown in orange at the 6σ level, confirming the presence of three copper ions.



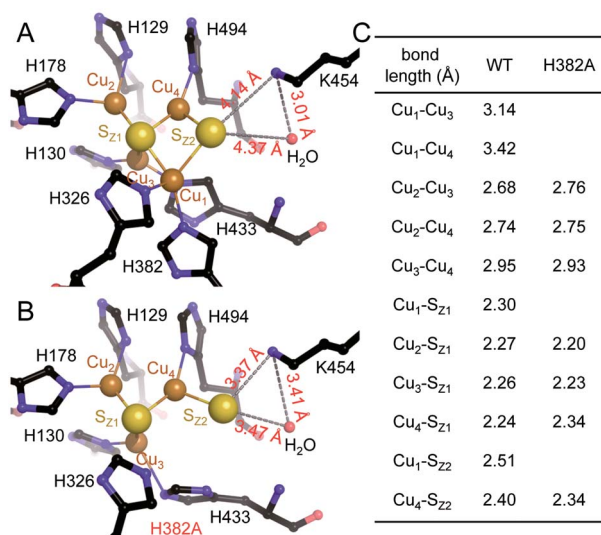


Fig. 3 Structural comparison of Cu<sub>2</sub> site and [3Cu:2S] site. (A) Structure of *holo*-N<sub>2</sub>OR isolated from *P. stutzeri* (PDB code: 3SBQ) shows Cu<sub>2</sub> site in the [4Cu:2S] state coordinated by seven histidine residues. K454 is too far from S<sub>22</sub> (4.14 Å) to form a bond. (B) In [3Cu:2S] site of variant H382A, residues H129, H130, H178, H326, H494 are in the same conformation as observed in the wild-type. However, H433 rotates by approximately 55° due to the space released by H382A. The distance between K454 and S<sub>22</sub> is close enough to form a weak hydrogen bond (3.37 Å). (C) Comparison of bond lengths for Cu<sub>2</sub> and [3Cu:2S] sites.

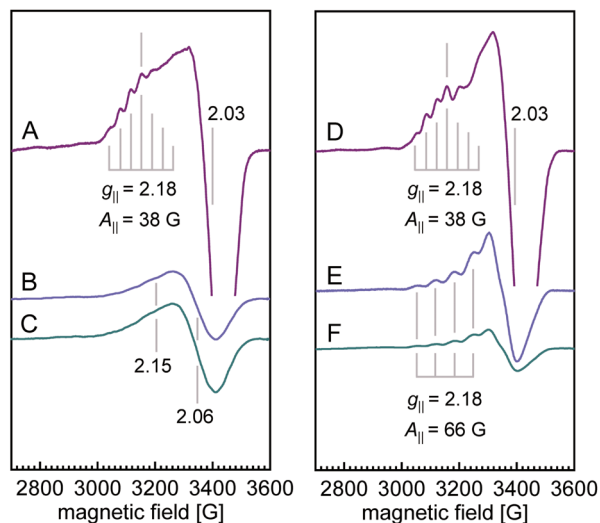


Fig. 4 X-band CW EPR spectra of WT *PsN<sub>2</sub>OR* (A–C) and variant H382A (D–F). Spectra for ferricyanide-oxidized (purple), ascorbate-reduced (blue), and dithionite-reduced (cyan) samples are shown, respectively. The intensities are normalized to spins per protein. Temperature, 10 K; power, 0.2 mW; microwave frequency, 9.635 GHz; modulation amplitude, 7.46 G.

peak in the  $g_{\parallel}$  region of H382A was more pronounced. In the spectrum of WT *PsN<sub>2</sub>OR*, reduction with ascorbate selectively removed the contribution of Cu<sub>A</sub>, leaving Cu<sub>Z</sub> in a di-cupric [2Cu<sup>2+</sup>:2Cu<sup>2+</sup>] state (Fig. 4B).<sup>4</sup> The further addition of dithionite reduced Cu<sub>Z</sub> to a [3Cu<sup>+</sup>:Cu<sup>2+</sup>] state (Fig. 4C).<sup>34</sup> In [2Cu<sup>+</sup>:2Cu<sup>2+</sup>]

Cu<sub>Z</sub>, the two oxidized coppers couple antiferromagnetically,<sup>4,35</sup> with a total spin of  $S = 0$ .<sup>21</sup> The EPR signal shown in Fig. 4B was derived from residual [3Cu<sup>+</sup>:Cu<sup>2+</sup>] Cu<sub>Z</sub>\* that was described to have lost sulfide S<sub>22</sub>.<sup>4,6,34</sup> Interestingly, EPR spectra of both ascorbate- and dithionite-reduced H382A showed a 4-line hyperfine splitting pattern in the  $g_{\parallel}$  region ( $g_{\parallel} = 2.18$ ,  $A_{\parallel} = 66$  G) (Fig. 4E and F), indicating the presence of a Cu(II) ion ( $S = 1/2$ , <sup>63/65</sup>Cu  $I = 3/2$ ) with its ground state in a 3d<sub>x<sup>2</sup>-y<sup>2</sup></sub>-derived molecular orbital,<sup>36,37</sup> and consistent with that of typical mononuclear type 1 (T1) copper as found in plastocyanin,<sup>37,38</sup> azurin,<sup>39–41</sup> cucumber basic protein,<sup>42</sup> as well as copper-containing nitrite reductase (NiR),<sup>43–45</sup> especially from fungal laccase<sup>46–48</sup> and Fet3p,<sup>49,50</sup> where Cu(II) is trigonal-planar coordinated by one cysteine and two histidine residues.

Reduction with dithionite (Fig. 4F) reduced the signal intensity to about 1/3 of that for the ascorbate-reduced sample (Fig. 4E), and also destabilized the cluster, as shown by the broad peak in the  $g = 2.3–2.4$  region (Fig. S12†). Therefore, the [3Cu:2S] cluster is very likely in a [2Cu<sup>+</sup>:Cu<sup>2+</sup>:2S<sup>2-</sup>]<sup>0</sup> state, with Cu<sub>4</sub> (Fig. 3B) as Cu(II), which is trigonally coordinated in the S(μ<sub>3</sub>-S)–N(His494)–S(μ<sub>2</sub>-S) plane.

Residue H326, the second ligand to Cu<sub>1</sub> in the Cu<sub>Z</sub> site (Fig. 3A), did not coordinate a metal in the [3Cu:2S] cluster (Fig. 3B). Thus, we expected the [3Cu:2S] cluster to be present in variant H326A as well. However, the H326A only contained a single Zn<sup>2+</sup> (Fig. S7†), indicating the stabilizing effect of H326 and H382 to the Cu<sub>Z</sub> site differs. We hypothesize that H326 is required already in the early stages of Cu<sub>Z</sub> maturation, so that the site will not assemble if this histidine residue is mutated. H382, in contrast, only seems come into play once the entire cluster is assembled. Our data do not reveal whether Cu<sub>Z</sub> is initially complete as a [4Cu:2S] cluster that is then prone to lose Cu<sub>1</sub> in the absence of the support by H382. Residue K454 (K397 in the case of N<sub>2</sub>OR from *M. hydrocarbonoclasticus*) was proposed to play a role in the catalytic cycle of N<sub>2</sub>OR by providing protons.<sup>34,51,52</sup> Our data show that it is also involved in the stabilization – and possibly assembly – of Cu<sub>Z</sub> through hydrogen-bonding interactions (Fig. 3B).

## Concluding remarks

Beyond these questions regarding the assembly of Cu<sub>Z</sub> *in vivo*, the [3Cu:2S] cluster in *PsN<sub>2</sub>OR* H382A also has interesting functional implications. In the variant, the cluster retains sulfide S<sub>22</sub>, but has it shifted towards residue K454, leading to UV/vis properties that fall between the forms I and II described earlier. Form II N<sub>2</sub>OR was proposed to contain a [4Cu:S] Cu<sub>Z</sub>\* center, requiring the loss of S<sub>22</sub> as a prerequisite for reductive activation.<sup>4</sup> Nevertheless the [4Cu:2S] Cu<sub>Z</sub> state has been consistently isolated from cells grown under denitrifying conditions (*i.e.* after having turned over *in vivo*).<sup>4,6,10,18,52,53</sup> The H382A variant may now help to reconcile these seemingly incompatible results, suggesting that S<sub>22</sub> can indeed change its position from ligating Cu<sub>1</sub> of Cu<sub>Z</sub> to the nearby K454 (similar sulfur-shift mechanism was envisaged by Moura and Pauleta).<sup>53</sup> This would leave both Cu<sub>1</sub> and Cu<sub>4</sub> with three remaining ligands, and thus with the opportunity to bind an additional



exogenous ligand, the substrate  $N_2O$ , in a 1,3-bridging fashion. This binding mode is similar to the one proposed by Moura and Solomon,<sup>52</sup> but does not require dissociation of  $S_{Z2}$  in accordance with our structural data.<sup>24</sup> It would also imply a binding mode of  $N_2O$  that is very much compatible with the  $N_2O$  binding site we observed at  $Cu_z$  after pressurizing crystals of the enzyme with the substrate gas.<sup>10</sup>

In particular, the UV-vis properties of the H382A variant highlight the fact that preparations of the enzyme that were typically assigned to a 'form II', or  $Cu_z^*$  species that implies a  $[4Cu:S]$  site may well be of a different nature. The loss of the charge transfer band at 550 nm that characterizes this form II may be rooted in the shift of  $S_{Z2}$  towards K454, without being fully lost from the cluster. This finding is also in line with the frequent observation of a less well-defined, elongate electron density feature at the  $Cu_1$ - $Cu_4$  edge of the  $Cu_z$  cluster in different published and unpublished structures. Such features were frequently interpreted as two  $H_2O$  ligands,<sup>9</sup> or inspired an originally suggested binding mode for  $N_2O$ <sup>54</sup> that was, however, never observed experimentally. The present data now offers an alternative rationalization for the reported spectroscopic features that may eventually lead to a unified picture of the structural and functional features of the unique and enigmatic  $Cu_z$  site.

## Conflicts of interest

There are no conflicts to declare.

## Acknowledgements

We thank the staff at beam lines X06SA and X06DA, Swiss Light Source, Villigen, CH, for excellent assistance with data collection, and Anne-Catherine Abel for help with the experiments. This work was supported by the European Research Council (grant 310656 to O. E.) and Deutsche Forschungsgemeinschaft (CRC 992, project no. 192904750).

## Notes and references

- 1 K. Butterbach-Bahl, E. M. Baggs, M. Dannenmann, R. Kiese and S. Zechmeister-Boltenstern, *Philos. Trans. R. Soc., B*, 2013, **368**, 20130122.
- 2 A. J. Thomson, G. Giannopoulos, J. Pretty, E. M. Baggs and D. J. Richardson, *Philos. Trans. R. Soc., B*, 2012, **367**, 1157–1168.
- 3 A. R. Ravishankara, J. S. Daniel and R. W. Portmann, *Science*, 2009, **326**, 123–125.
- 4 E. M. Johnston, S. Dell'Acqua, S. Ramos, S. R. Pauleta, I. Moura and E. I. Solomon, *J. Am. Chem. Soc.*, 2014, **136**, 614–617.
- 5 S. R. Pauleta, S. Dell'Acqua and I. Moura, *Coord. Chem. Rev.*, 2013, **257**, 332–349.
- 6 T. Rasmussen, B. C. Berks, J. N. Butt and A. J. Thomson, *Biochem. J.*, 2002, **364**, 807–815.
- 7 K. Brown, M. Tegoni, M. Prudencio, A. S. Pereira, S. Besson, J. J. Moura, I. Moura and C. Cambillau, *Nat. Struct. Biol.*, 2000, **7**, 191–195.
- 8 K. Brown, K. Djinovic-Carugo, T. Haltia, I. Cabrito, M. Saraste, J. J. G. Moura, I. Moura, M. Tegoni and C. Cambillau, *J. Biol. Chem.*, 2000, **275**, 41133–41136.
- 9 K. Paraskevopoulos, S. V. Antonyuk, R. G. Sawers, R. R. Eady and S. S. Hasnain, *J. Mol. Biol.*, 2006, **362**, 55–65.
- 10 A. Pomowski, W. G. Zumft, P. M. Kroneck and O. Einsle, *Nature*, 2011, **477**, 234–237.
- 11 L. K. Schneider and O. Einsle, *Biochemistry*, 2016, **55**, 1433–1440.
- 12 J. A. Farrar, F. Neese, P. Lappalainen, P. M. H. Kroneck, M. Saraste, W. G. Zumft and A. J. Thomson, *J. Am. Chem. Soc.*, 1996, **118**, 11501–11514.
- 13 D. R. Gamelin, D. W. Randall, M. T. Hay, R. P. Houser, T. C. Mulder, G. W. Canters, S. de Vries, W. B. Tolman, Y. Lu and E. I. Solomon, *J. Am. Chem. Soc.*, 1998, **120**, 5246–5263.
- 14 M. E. Llases, M. N. Lisa, M. N. Morgada, E. Giannini, P. M. Alzari and A. J. Vila, *FEBS J.*, 2020, **287**, 749–762.
- 15 C. L. Coyle, W. G. Zumft, P. M. H. Kroneck, H. Körner and W. Jakob, *Eur. J. Biochem.*, 1985, **153**, 459–467.
- 16 C. Carreira, M. M. C. Dos Santos, S. R. Pauleta and I. Moura, *Bioelectrochemistry*, 2020, **133**, 107483.
- 17 W. G. Zumft and P. M. H. Kroneck, *Adv. Microb. Physiol.*, 2007, **52**, 107–227.
- 18 E. M. Johnston, S. Dell'Acqua, S. R. Pauleta, I. Moura and E. I. Solomon, *Chem. Sci.*, 2015, **6**, 5670–5679.
- 19 W. G. Zumft, *Microbiol. Mol. Biol. Rev.*, 1997, **61**, 533–616.
- 20 L. K. Schneider, A. Wüst, A. Pomowski, L. Zhang and O. Einsle, *Met. Ions Life Sci.*, 2014, **14**, 177–210.
- 21 S. R. Pauleta, M. S. P. Carepo and I. Moura, *Coord. Chem. Rev.*, 2019, **387**, 436–449.
- 22 M. A. McGuirl, J. A. Bollinger, N. Cosper, R. A. Scott and D. M. Dooley, *J. Biol. Inorg. Chem.*, 2001, **6**, 189–195.
- 23 S. P. Bennett, M. J. Soriano-Laguna, J. Bradley, D. A. Svistunenko, D. J. Richardson, A. J. Gates and N. E. Le Brun, *Chem. Sci.*, 2019, **10**, 4985–4993.
- 24 L. Zhang, A. Wüst, B. Prasser, C. Müller and O. Einsle, *Proc. Natl. Acad. Sci. U. S. A.*, 2019, **116**, 12822–12827.
- 25 S. Dell'Acqua, S. R. Pauleta, J. J. Moura and I. Moura, *Philos. Trans. R. Soc., B*, 2012, **367**, 1204–1212.
- 26 J. M. Charnock, A. Dreusch, H. Körner, F. Neese, J. Nelson, A. Kannt, H. Michel, C. D. Garner, P. M. Kroneck and W. G. Zumft, *Eur. J. Biochem.*, 2000, **267**, 1368–1381.
- 27 P. Chen, I. Cabrito, J. J. Moura, I. Moura and E. I. Solomon, *J. Am. Chem. Soc.*, 2002, **124**, 10497–10507.
- 28 P. M. H. Kroneck, *J. Biol. Inorg. Chem.*, 2018, **23**, 27–39.
- 29 P. A. Williams, N. J. Blackburn, D. Sanders, H. Bellamy, E. A. Stura, J. A. Fee and D. E. McRee, *Nat. Struct. Biol.*, 1999, **6**, 509–516.
- 30 A. I. Graham, S. Hunt, S. L. Stokes, N. Bramall, J. Bunch, A. G. Cox, C. W. McLeod and R. K. Poole, *J. Biol. Chem.*, 2009, **284**, 18377–18389.



- 31 I. Petit-Hartlein, K. Rome, E. de Rosny, F. Molton, C. Duboc, E. Gueguen, A. Rodrigue and J. Coves, *Biochem. J.*, 2015, **472**, 205–216.
- 32 C. A. Blindauer, *Chem. Commun.*, 2015, **51**, 4544–4563.
- 33 I. Dokmanic, M. Sikic and S. Tomic, *Acta Crystallogr., Sect. D: Biol. Crystallogr.*, 2008, **64**, 257–263.
- 34 S. Ghosh, S. I. Gorelsky, S. DeBeer George, J. M. Chan, I. Cabrito, D. M. Dooley, J. J. G. Moura, I. Moura and E. I. Solomon, *J. Am. Chem. Soc.*, 2007, **129**, 3955–3965.
- 35 S. I. Gorelsky, S. Ghosh and E. I. Solomon, *J. Am. Chem. Soc.*, 2006, **128**, 278–290.
- 36 E. I. Solomon and R. G. Hadt, *Coord. Chem. Rev.*, 2011, **255**, 774–789.
- 37 E. I. Solomon, R. K. Szilagy, S. D. George and L. Basumallick, *Chem. Rev.*, 2004, **104**, 419–458.
- 38 J. M. Guss and H. C. Freeman, *J. Mol. Biol.*, 1983, **169**, 521–563.
- 39 H. B. Gray, B. G. Malmström and R. J. P. Williams, *J. Biol. Inorg. Chem.*, 2000, **5**, 551–559.
- 40 H. Nar, A. Messerschmidt, R. Huber, M. Vandekamp and G. W. Canters, *J. Mol. Biol.*, 1991, **218**, 427–447.
- 41 C. M. Groeneveld, R. Aasa, B. Reinhammar and G. W. Canters, *J. Inorg. Biochem.*, 1987, **31**, 143–154.
- 42 L. B. LaCroix, D. W. Randall, A. M. Nersissian, C. W. G. Hoitink, G. W. Canters, J. S. Valentine and E. I. Solomon, *J. Am. Chem. Soc.*, 1998, **120**, 9621–9631.
- 43 L. B. LaCroix, S. E. Shadle, Y. N. Wang, B. A. Averill, B. Hedman, K. O. Hodgson and E. I. Solomon, *J. Am. Chem. Soc.*, 1996, **118**, 7755–7768.
- 44 K. Olesen, A. Veselov, Y. W. Zhao, Y. S. Wang, B. Danner, C. P. Scholes and J. P. Shapleigh, *Biochemistry*, 1998, **37**, 6086–6094.
- 45 H. Iwasaki, S. Noji and S. Shidara, *J. Biochem.*, 1975, **78**, 355–361.
- 46 A. E. Palmer, D. W. Randall, F. Xu and E. I. Solomon, *J. Am. Chem. Soc.*, 1999, **121**, 7138–7149.
- 47 A. Messerschmidt and R. Huber, *Eur. J. Biochem.*, 1990, **187**, 341–352.
- 48 D. M. Dooley, J. Rawlings, J. H. Dawson, P. J. Stephens, L. E. Andreasson, B. G. Malmström and H. B. Gray, *J. Am. Chem. Soc.*, 1979, **101**, 5038–5046.
- 49 T. E. Machonkin, L. Quintanar, A. E. Palmer, R. Hassett, S. Severance, D. J. Kosman and E. I. Solomon, *J. Am. Chem. Soc.*, 2001, **123**, 5507–5517.
- 50 A. B. Taylor, C. S. Stoj, L. Ziegler, D. J. Kosman and P. J. Hart, *Proc. Natl. Acad. Sci. U. S. A.*, 2005, **102**, 15459–15464.
- 51 S. Bagherzadeh and N. P. Mankad, *Chem. Commun.*, 2018, **54**, 1097–1100.
- 52 E. M. Johnston, C. Carreira, S. Dell'Acqua, S. G. Dey, S. R. Pauleta, I. Moura and E. I. Solomon, *J. Am. Chem. Soc.*, 2017, **139**, 4462–4476.
- 53 C. Carreira, R. F. Nunes, O. Mestre, I. Moura and S. R. Pauleta, *J. Biol. Inorg. Chem.*, 2020, **25**, 927–940.
- 54 S. Ghosh, S. I. Gorelsky, P. Chen, I. Cabrito, J. J. G. Moura, I. Moura and E. I. Solomon, *J. Am. Chem. Soc.*, 2003, **125**, 15708–15709.

